

Kinetics of Protein Degradation and Physical Changes in Thermally Processed Atlantic Salmon (*Salmo salar*)

Mahmoudreza Ovissipour^{1,2} · Barbara Rasco² · Juming Tang¹ · Shyam Sablani¹

Received: 23 March 2017 / Accepted: 10 July 2017 / Published online: 22 July 2017
© Springer Science+Business Media, LLC 2017

Abstract Protein denaturation is the main reason for physicochemical changes in muscle foods during thermal processing. The purpose of this study was to understand the kinetics of quality degradation and protein denaturation of Atlantic salmon (*Salmo salar*) during thermal pasteurization. Findings indicate that cook loss, area shrinkage, and protein denaturation parameters (both dielectric loss and differential scanning calorimetry (DSC) studies) were best fitted to a first-order reaction. In addition, color parameters followed zero-order kinetics. Fourier transform infrared spectroscopy (FTIR) results showed that increasing heating time and temperature reduced the α -helix peak, indicating protein denaturation. At the same time, the β -sheet peak intensity increased, which is related to protein aggregation. Correlation loading plots from FTIR spectra showed that protein denaturation was dominant below 75 °C. Above this transition temperature, protein denaturation occurred rapidly and protein aggregation became more obvious. The dielectric properties in cooked salmon at different times and temperature increased with increasing heating time and temperature, while penetration depth decreased significantly ($P < 0.05$). The kinetics of protein denaturation from DSC showed that the activation energy of 300.6 kJ/mol and k_0 was $1.1 \times 10^{42} \text{ min}^{-1}$. Our findings on kinetic data from protein denaturation and physical changes may be used to improve the processing schedule in the production of safe, high-quality pasteurized salmon.

Keywords Atlantic salmon · Protein denaturation · Physical changes · Dielectric properties · FTIR · DSC

Introduction

Atlantic salmon is one of the most important seafood products in the world, with 2,326,288 t production annually (FAO 2014). Heat treatment is often used to control bacteria, fungi, and viruses and inactivate enzymes in order to produce safe products for consumers (Ling et al. 2015). However, thermal processing of food may cause severe quality deterioration, particularly in high-protein content foods. Degradation in color and texture, nutrient loss, cook loss (weight loss), and shrinkage can reduce consumer acceptance (Ovissipour et al. 2013; Ling et al. 2015). Although heating is one of the most common methods to control food safety and extend shelf-life, new strategies are needed to reduce the amount of heat required for microbial control to maintain quality (Ovissipour et al. 2013).

Most changes in physical quality attributes in salmon during thermal processing are due to protein denaturation. Protein denaturation reduces water-holding capacity, shrinks muscle fibers, and causes connective tissue degradation, leading to a harder and more compact tissue texture (Kong et al. 2007a; Skipnes et al. 2011). Color is a physical attribute that influences consumer acceptability. During thermal processing, color is affected by several mechanisms, including degradation of pigments, oxidation of ascorbic acid, and enzymatic and non-enzymatic browning (Kong et al. 2007a,b; Ovissipour et al. 2013; Ling et al. 2015). Texture is characterized as a series of physical parameters related to the composition and structure of the food, perceived in the mouth. Compression and puncture tests are the two most important and common methods to measure mechanical properties of foods (Kong et al. 2007a;

✉ Shyam Sablani
ssablani@wsu.edu

¹ Department of Biological Systems Engineering, Washington State University, Pullman, WA 99164, USA

² School of Food Science, Washington State University, Pullman, WA 99164, USA

Ovissipour et al. 2013). Cook loss and shrinkage of meat and fish muscles are two key quality attributes resulting from heat-induced protein denaturation through shrinkage of myofibers and collagen and the denaturation of sarcoplasmic proteins (Cao et al. 2016).

Due to structural differences between finfish and mammalian muscle, the effect of thermal processing is generally detrimental to seafood (Skipnes et al. 2008; Ovissipour et al. 2013).

Another important quality attribute is the protein structure and degradation kinetics during thermal processing. Studies show that protein denaturation and aggregation are mainly responsible for cook loss and physical changes during thermal processing of seafood (Ofstad et al. 1996; Kong et al. 2007a; Skipnes et al. 2008; Dima et al. 2012; Ovissipour et al. 2013; Verhaeghe et al. 2016). In thermal processing, protein degradation starts with protein denaturation and continues with protein aggregation, resulting in shrinkage of myofibrils and expulsion of water (Kong et al. 2007a). Several methods have been used to study protein denaturation and structural changes of protein-based foods in response to salt, high pressure, aging, and thermal processing. These methods include Fourier transform infrared spectroscopy (FTIR), differential scanning calorimetry (DSC), and dielectric properties. Studies indicate different temperatures of denaturation for different proteins. For example, Skipnes et al. (2008) used DSC to find the temperature of protein denaturation in Atlantic cod (*Gadus morhua*) which were 44, 57, and 76 °C for myosin, sarcoplasmic proteins, and actin, respectively. Ofstad et al. (1996) reported that the temperatures of proteins denaturation are 45, 65, and 78 °C in Atlantic salmon (*Salmo salar*). Ojagh et al. (2011) studied the effect of high pressure on Atlantic salmon protein structure using FTIR, finding that protein denaturation and aggregation can be studied by focusing on the secondary derivative of the FTIR spectra. Dielectric properties were also applied to study protein denaturation in various foods, including salmon, cod and chicken (Bircan and Barringer 2002), salmon (Wang et al. 2008), and egg protein (Wang et al. 2009). This kinetic study on protein structural changes during thermal processing will elucidate the mechanisms behind the physical changes of food in response to thermal processing. Many kinetic studies have explored thermal inactivation of microorganisms and quality changes (Kong et al. 2007a; Skipnes et al. 2008; Dima et al. 2012; Ovissipour et al. 2013; Mao et al. 2016; Verhaeghe et al. 2016). To our knowledge, there is no data on the thermal protein degradation kinetics of Atlantic salmon muscle that is pasteurized at different times and temperatures. There is also no systematic study of protein degradation using FTIR and dielectric properties. Hence, this study aims to determine the kinetics of physical quality changes and protein degradation in Atlantic salmon during thermal processing at pasteurization temperature range. We also explored the relationship between different protein

degradation measurement methods and their correlation with physical quality changes.

Materials and Methods

Thermal Treatment

Three days post-harvest, fresh Atlantic salmon (*S. salar*) fillets were purchased from a local retailer in Pullman, WA and transferred to the lab within 30 min. They were kept at room temperature for 30 min to equilibrate to approximately 22 °C. Pasteurization treatments were conducted at different times and temperatures (Table 1), based on target bacteria and industry requirements. Selected temperatures were 55, 65, 75, 85, and 90 °C for various times to provide equivalent lethality and sufficient heating to inactivate norovirus, *Listeria monocytogenes*, and *Clostridium botulinum* type E (Gaze et al. 2006; Gibson and Schwab 2011) (Table 1) ($N = 4$).

Next, 12 ± 1 g of Atlantic salmon white muscle from the mid-part of the fish fillet (between the lateral line and dorsal fin) was placed in the custom built cylindrical aluminum test cell which was previously used for the kinetic study of muscle foods (Kong et al. 2007a,b; Ovissipour et al. 2013). Come-up time, defined as the required time required for the center of the sample to reach within 1 °C of the total temperature rise, was determined using a 0.1-mm-diameter copper-constantan thermocouple (type T) inserted through a rubber gland in the container lid. After heating, the sample cells were removed from the water bath and immersed in an ice water mixture to immediately cool the fish muscle. After cooling, the Atlantic salmon muscle samples were patted dry with a filter paper and weighed.

Color Measurement

Color (L , a , b) was measured before and after heat treatment using a tristimulus spectrophotometer (model CM-5, Konica Minolta Sensing Inc., Japan) recording L^* (lightness), a^* (redness), and b^* (yellowness). Four measurements were conducted for each sample.

$$\Delta E = \sqrt{(L_0 - L_t)^2 + (a_0 - a_t)^2 + (b_0 - b_t)^2} \quad (1).$$

Table 1 Experimental heating conditions

Temperature (°C)	Heating time (min)						
55	9	20	30	40	50	60	70
65	1	4	9	15	20	25	30
75	1	3	5	8	10	13	15
85	1	2	4	6	7	9	10
90	1	2	4	8	10	12	14

Cook Loss

Cook loss was calculated according to Ovissipour et al. (2013) with the following equation:

$$\text{Cook loss} = \left(\frac{\text{weight of raw sample} - \text{Weight of cooked sample}}{\text{weight of raw sample}} \right) \times 100 \quad (2)$$

Area Shrinkage

Area shrinkage was calculated based on the area of the individual sample before and after thermal processing, using ImageJ software Version 1.47a (National Institute of Health, USA). The shrinkage ratio was calculated as:

$$\text{Area shrinkage ratio} = \left(\frac{\text{area of raw sample} - \text{area of cooked sample}}{\text{area of raw sample}} \right) \times 100 \quad (3)$$

Mechanical Properties

Compression force (N) was measured with a stainless-steel puncture probe (5 mm internal diameter, 35 mm probe length), using a Texture Analyzer TA-XT2 (Stable Micro Systems Ltd., Surrey, UK) equipped with a 5-kg load cell. Atlantic salmon muscle samples (50 mm × 20 mm × 5 mm) were equilibrated to room temperature (ca. 22 °C) within approximately 30 min. Compression at different locations on the fillet portion was then measured. The traveling speed for the probe was set at 1 mm/s, over a distance of 3 mm (60% of the sample). Texture Expert for Windows (version 1.15, Stable Micro Systems Ltd.) software was used to record and analyze the force–time graphs for each sample. The compression force was defined as the peak maximum height in the force–time profile.

Fourier Transform Infrared Spectroscopy

Salmon muscle blocks (1 cm × 0.5 cm × 0.2 cm) were prepared from the raw and heat-treated fish at different times and temperatures. FTIR spectral features of each salmon muscle sample were collected using a Thermo Nicolet Avatar 360 FTIR spectrometer (Thermo Electron Inc., San Jose, CA, USA). Samples were placed in direct contact with the ATR crystal cell and spectra were taken between 4000 and 400 cm⁻¹. Ten spectra were collected at room temperature

(ca. 22 °C) for each sample in five replicates ($N = 5$) with a total of 50 spectra for each sample at different locations.

DSC Analysis

Two DSC studies were carried out, which in the first part of the study, the degree of protein denaturation of thermally processed Atlantic salmon based on the scheduled time and temperature (Table 1) was determined. Results were used to interpret findings from the FTIR and dielectric property experiments on protein denaturation and aggregation. In the second part of the study, the kinetics of protein denaturation and aggregation were determined by designing new time and temperature protocols (66, 68, 70, 72, and 74 °C). DSC was performed at a heating rate of 10 °C/min over the range from 0 to 100 °C, using a modulated differential scanning calorimeter (MDSC, Q2000, TA Instruments, Waters LLC., New Castle, DE, USA). An empty pan was used as a reference, and a 1-min equilibration at 0 °C was conducted before each run. Fifteen milligrams of each sample was sealed into aluminum pans (capacity 30 μL) ($N = 3$). Residual denaturation enthalpy (ΔH) (J/g), which is the area under the denaturation peak, was used to determine the kinetics of protein denaturation (Skipnes et al. 2008). The area was calculated with Universal Analysis 2000 software (TA Instruments, Waters LLC., New Castle, DE, USA).

Dielectric Properties

An open-ended coaxial probe (Hewlett Packard 85070B dielectric probe kit) was used to measure the dielectric properties of preheated fish muscle samples according to Table 1 time and temperature schedule, at 22 °C. An Agilent E5071C ENA network analyzer kit (Agilent Technologies, Palo Alto, CA, USA) was used, including an open load, a short load, and a 50-Ω load to calibrate the network. The probe was also calibrated by air, short circuit, and deionized water at room temperature. The instrument was set up to measure the dielectric constant and loss factor in a frequency range of 1 to 1800 MHz.

Power Penetration Depth

Power penetration depth is one of the most important dielectric property parameters in the thermal processing of food. The penetration depth was calculated with the following equation (Buffler 1993):

$$dp = \frac{c}{2\pi f \sqrt{2\varepsilon' \left[\sqrt{\left(\frac{\varepsilon''}{\varepsilon'}\right)^2 + 1} - 1 \right]}} \quad (4)$$

where c is the rate of electromagnetic wave in free space and equals to 3×10^8 m/s and f is the frequency (Hz).

Kinetic Analysis

Reaction rates for quality degradation (C) in isothermal conditions are expressed in the following equation (Kong et al. 2007a):

$$\frac{dC}{dt} = -k(C)^n \quad (5)$$

where k is the rate constant, C is the quality at time t , and n is the order of reaction. To find the best empirical relationship, quality data were analyzed using zero-, first-, and second-order kinetic models in Eqs. (6)–(8):

Zero-order:

$$C_t = C_0 - k \cdot t \quad (6)$$

First-order:

$$\ln \frac{C_t}{C_0} = -k \cdot t \quad (7)$$

Second-order:

$$k_t = \frac{1}{C_t} - \frac{1}{C_0} \quad (8)$$

where C_0 is the initial amount of the quality at time zero, C_t is the value at time t , and k is the rate constant. In addition, Arrhenius equation was used to determine the degradation rate constant (k) on temperature, which is described as follows:

$$k = k_0 \exp \left[-\frac{E_a}{RT} \right] \quad (9)$$

where E_a is the activation energy of the reaction (kJ/mol), R is universal gas constant (8.3145 J/mol/K), T is the absolute temperature (K), and k_0 is the frequency factor (per min). By applying Eq. (9) to a reaction, a plot of the rate constant on semi-logarithmic scale as a function of reciprocal absolute temperature ($1/T$) should yield a straight line. The activation energy can be determined as the slope of the line multiplied by the gas constant R .

Statistical and FTIR Data Analysis

A one-way analysis of variance (ANOVA) (Duncan multiple test) was applied to determine the significant differences among treatments using SPSS software 16.0 (SPSS Inc., Chicago, IL) at a probability level of $P < 0.05$. FTIR spectral analyses were carried out using OMNIC (Thermo Electron

Inc.). Pre-processing of algorithms was also performed, including automatic baseline correction, smoothing, and normalization. Second derivatives were provided to improve the resolution of the spectral bands by applying a nine-point Savitzky-Golay filter (Bocker et al. 2008). After pre-processing, a principal component analysis (PCA) was developed for each temperature for the second derivative amide I region between 1700 and 1600 cm^{-1} , which is related to the protein secondary structure, using Matlab R2010a (MathWorks, Inc. Natick, MA, USA). Contour plots were prepared using Minitab® 14 (Minitab Inc., PA, USA).

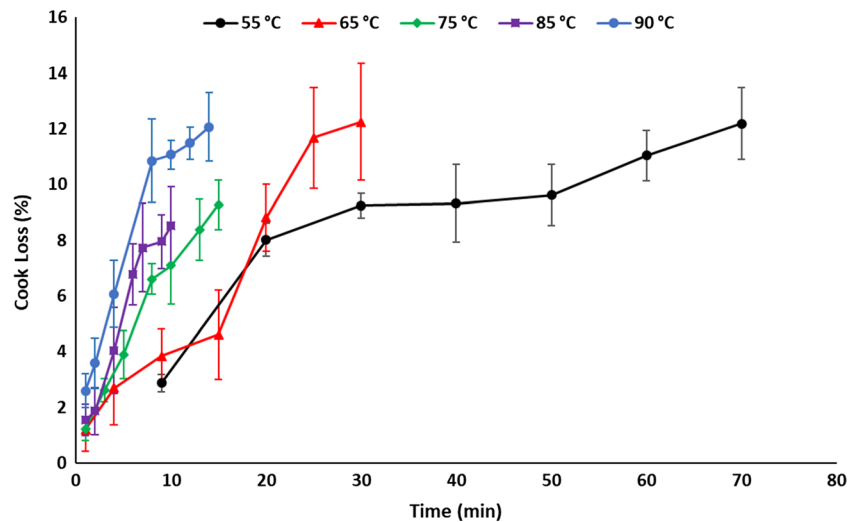
Results and Discussion

Cook Loss and Area Shrinkage

Results show that cook loss increased significantly ($P < 0.05$) with increasing time and temperature of thermal processing (Fig. 1). The majority of the cook loss for each temperature occurred in the first few minutes of heating. This accords with previous results for Atlantic cod (*G. morhua*) (Skipnes et al. 2011), pink salmon (*Onchorynchus gorbusha*) (Kong et al. 2007a), blue mussel (*Mytilus edulis*) (Ovissipour et al. 2013), grass carp (*Ctenopharyngodon idellus*) (Cao et al. 2016), and ground beef (Niu et al. 2015). By increasing the heating time, the slope of the cook loss eventually decreased. After 10 min of heating, the cook loss was 3% (55 °C), 4% (65 °C), 7% (75 °C), 8.5% (85 °C), and 11% (90 °C). More than 20% of the total cook loss occurred within 2 to 4 min after heating at higher temperatures, while, at 55 °C, cook loss occurred within 9 min. Kong et al. (2007a) reported that the 40% of the cook loss occurred in 2 to 3 min after heating pink salmon at 100, 111, 121, and 131 °C. Ovissipour et al. (2013) reported that more than 60% of the cook loss occurred within 5 min after heating whole blue mussel, which contains much less myofibrillar protein and had a lower amount of connective tissue than Atlantic salmon.

The cook loss kinetic reaction indicated a first-order reaction, following a similar trend as in our prior work (Kong et al. 2007a; Ovissipour et al. 2013). Table 2 summarizes the rate constants for five temperatures, E_a , k_0 value, and coefficient of correlation. The activation energy was 54.9 kJ/mol, similar to that of beef (54.93 kJ/mol) (Bertola et al. 1994) and blue mussel (55.6 kJ/mol) (Ovissipour et al. 2013) but higher than that of pink salmon (37.0 kJ/mol) (Kong et al. 2007a). Thermal processing results in muscle protein denaturation and aggregation, which is the main reason for moisture loss due to changes in the functional properties of protein (Ovissipour et al. 2013; Cao et al. 2016). More than 85% of the cook loss is moisture, while the remainder is composed of lipids, collagen or gelatin, muscle fragments, and aggregated

Fig. 1 Cook loss in Atlantic salmon thermally treated at different times and temperatures



sarcoplasmic proteins (Kong et al. 2007a; Skipnes et al. 2007, 2011; Ovissipour et al. 2013).

Results for area shrinkage also followed first-order kinetics. Table 2 also shows the kinetic parameters for area shrinkage. During thermal processing, the diameter of muscle fibers and the length of the sarcomere shrink due to expelled water, soluble proteins, and fats and protein denaturation (Bertola et al. 1994; Kong et al. 2007a,b; Ovissipour et al. 2013). Since both cook loss and area shrinkage are related to protein denaturation, a high correlation has been reported for fish muscle (Ofstad et al. 1996), beef (Palka and Daun 1999), pork (Barbera and Tassone 2006), pink salmon (Kong et al. 2007a), and blue mussel (Ovissipour et al. 2013). In this study, the correlation between cook loss and area shrinkage for all temperatures was positive, with a coefficient of correlation of over 80%.

Color Changes

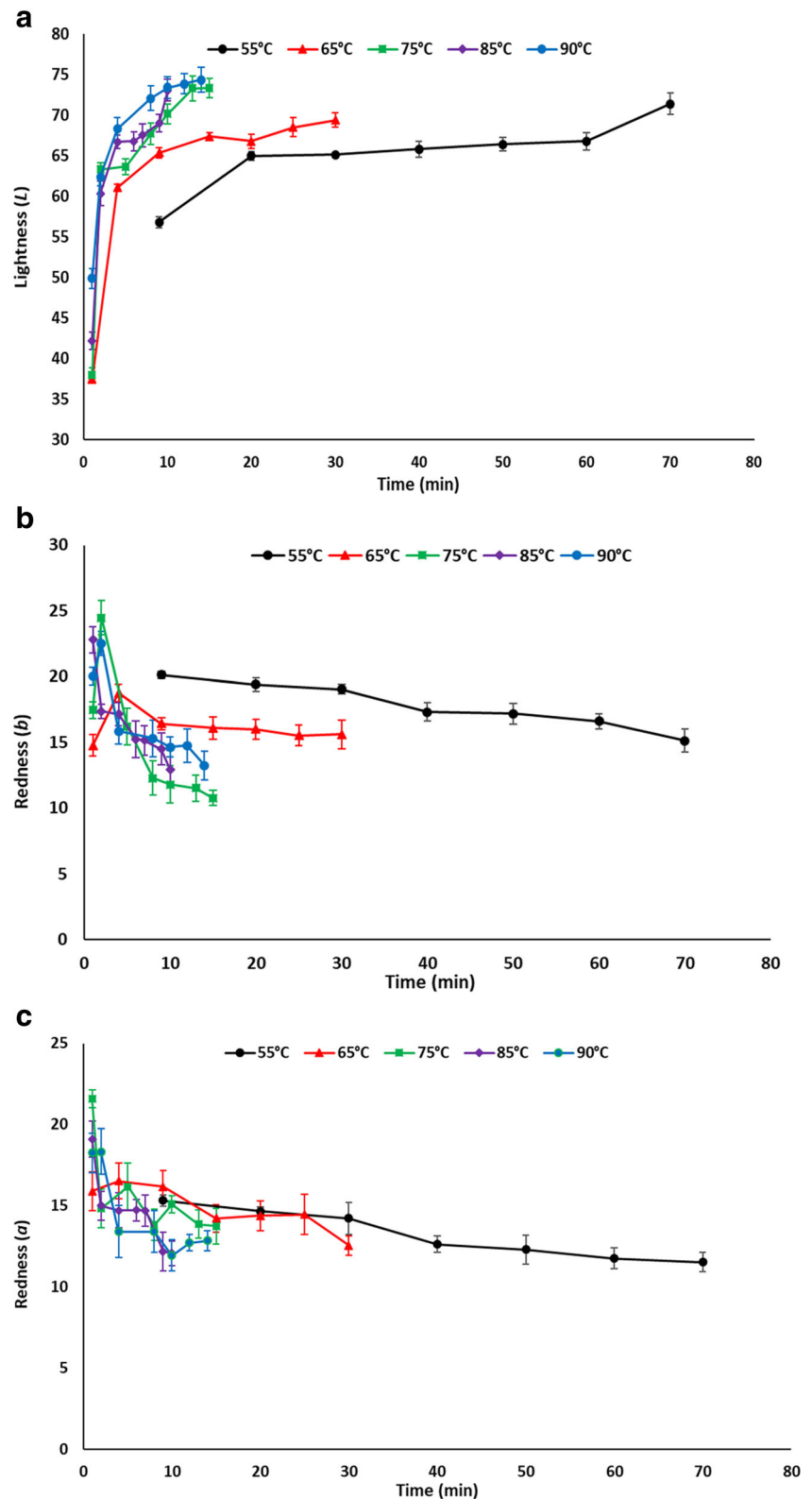
During thermal processing of Atlantic salmon, the pink color of fish muscle was masked, with a rapid increase in the *L* value and sharp decrease in the *a* and *b* values (*P* < 0.05) at all

temperatures (Fig. 2). In addition, the kinetics of color parameters were zero-order. Similar trends have been reported for Pacific chum salmon (*Oncorhynchus keta*) heated at 60 to 100 °C (Bhattacharya et al. 1994) and pink salmon heated at 100 to 131.1 °C (Kong et al. 2007a). Kong et al. (2007a) reported a zero-order kinetic reaction, with the *E_a* of 88.0, 73.8, and 99.5 kJ/mol for *L*, *b*, and ΔE values, which differed slightly from our findings. This may be due to different color measurement methods, a difference in the initial color of the fish species, and the range in heating temperatures. However, our findings fell in the range of quality kinetic degradation (60–120 kJ/mol) (Kong et al. 2007a) (Table 3). Kong et al. (2007a) also reported a rapid whitening followed by a browning phase during thermal processing of pink salmon at 100 to 131.1 °C. Whitening is due to the quick denaturation of heme proteins and carotenoid oxidation, while the browning phase is related to the Maillard reaction between sugars, fish proteins, and amines (Haard 1992). In this study, the browning phase was not observed, due to lower tested temperatures compared to Kong et al. (2007a). The browning phase usually appears as processing temperature and time increase (Whistler and Daniel 1985).

Table 2 First-order kinetic parameters for cook loss and area shrinkage of Atlantic salmon after heat treatment at different temperatures

Parameter	Temperature (°C)	<i>k</i> (min ⁻¹)	<i>R</i> ²	<i>E_a</i> (kJ/mol)	<i>k</i> ₀ (min ⁻¹)	<i>R</i> ²
Cook loss	55	0.0012	0.7903	54.9	930	0.8738
	65	0.0043	0.9388			
	75	0.007	0.9813			
	85	0.0089	0.9228			
	90	0.0092	0.9471			
Area shrinkage	55	0.0015	0.9388	106.9	7.08 × 10 ¹⁰	0.8892
	65	0.0049	0.8779			
	75	0.0085	0.9491			
	85	0.0122	0.9745			
	90	0.0133	0.9563			

Fig. 2 Changes in color parameters during thermal processing of Atlantic salmon. **a** *L* value. **b** *b* value. **c** *c* value



Mechanical Properties

Figure 3 displays the change in mechanical properties. Changes in the texture profile indicate that at all temperatures, two peaks

divided the texture profile into four sections. Kong et al. (2007a) observed the same pattern for heated pink salmon at 100 to 131.1 °C and explained the four sections as follows: rapid toughening, rapid tenderization, slow toughening, and slow

Table 3 Zero-order kinetic parameters for color parameters of Atlantic salmon after heat treatment at different temperatures

Parameter	Temperature (°C)	k (min ⁻¹)	R^2	E_a (kJ/mol)	k_0 (min ⁻¹)	R^2
L	55	0.17	0.8160	67.3	7.6×10^6	0.9569
	65	0.24	0.8064			
	75	0.78	0.9700			
	85	1.34	0.9050			
	90	1.42	0.9233			
b	55	0.09	0.7278	57.5	1.4×10^5	0.6018
	65	0.10	0.8767			
	75	1.03	0.7943			
	85	0.54	0.9523			
	90	0.50	0.8582			
ΔE	55	0.133	0.5982	81.8	2.3×10^9	0.8425
	65	0.94	0.8135			
	75	1.73	0.5337			
	85	3.53	0.5768			
	90	2.32	0.8606			

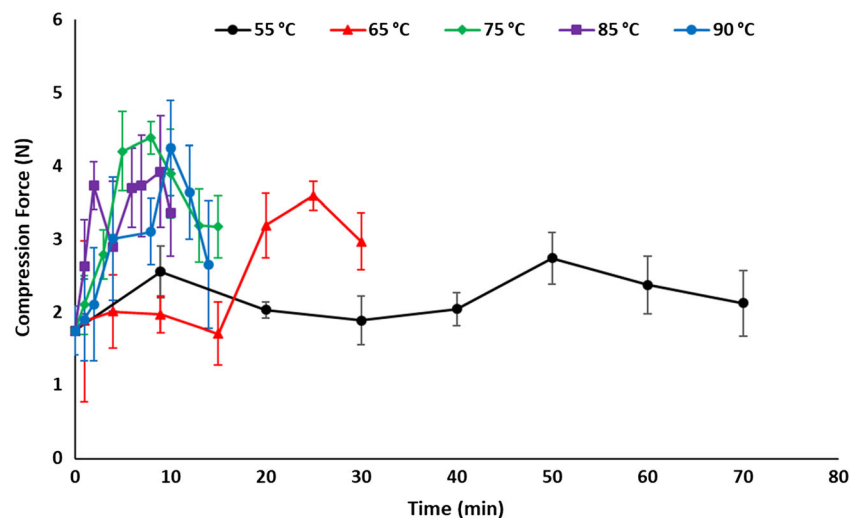
tenderization. They also note that optimum cooking time in terms of texture is between the first and second peak. Since the temperatures of protein denaturation in fish muscle were reported between 40 and 80 °C (Skipnes et al. 2008), textural changes are likely caused by the denaturation of myofibrillar proteins and the gelation of collagen (Kong et al. 2007a). For fish muscle, myosin and actin are more important in gelation due to lower collagen content (Skipnes et al. 2011). As temperature increased, the toughening phase time decreased. This indicates that at higher temperatures, the protein denaturation rate is faster than protein aggregation. This accords with our findings from the biochemical study (FTIR, DSC, and dielectric properties).

FTIR Spectroscopy

Amide I (1700–1600 cm⁻¹) is the most dominant band in myofiber spectrum and the most useful for studying the

secondary structure of protein. This is due to its sensitivity to hydrogen-bonding patterns, dipole-dipole interaction, and the geometry of the polypeptide backbone (Astruc et al. 2012; Carton et al. 2009). This is mainly assigned to a C=O stretching vibration and minor in-plane N-H bending and C-N stretching vibration. Changes in spectra in the amide I region due to heating or salting have been studied in various muscle foods, including brined Atlantic salmon (Carton et al. 2009; Bocker et al. 2008), pressurized and heated (40 °C) Atlantic salmon (Ojagh et al. 2011), cooked pork (Bertram et al. 2006; Wu et al. 2006), aged beef (Kirschner et al. 2004), and heated beef (Astruc et al. 2012).

In this study, amide I in the original spectra had a maximum absorbance of 1638 cm⁻¹ in raw Atlantic salmon. This shifted to lower frequencies as heating temperature and time increased. The minimum frequency was 1626 cm⁻¹ in samples heated at 90 °C for 14 min. The peak intensity decreased significantly as

Fig. 3 Changes in compression force during thermal processing of Atlantic salmon

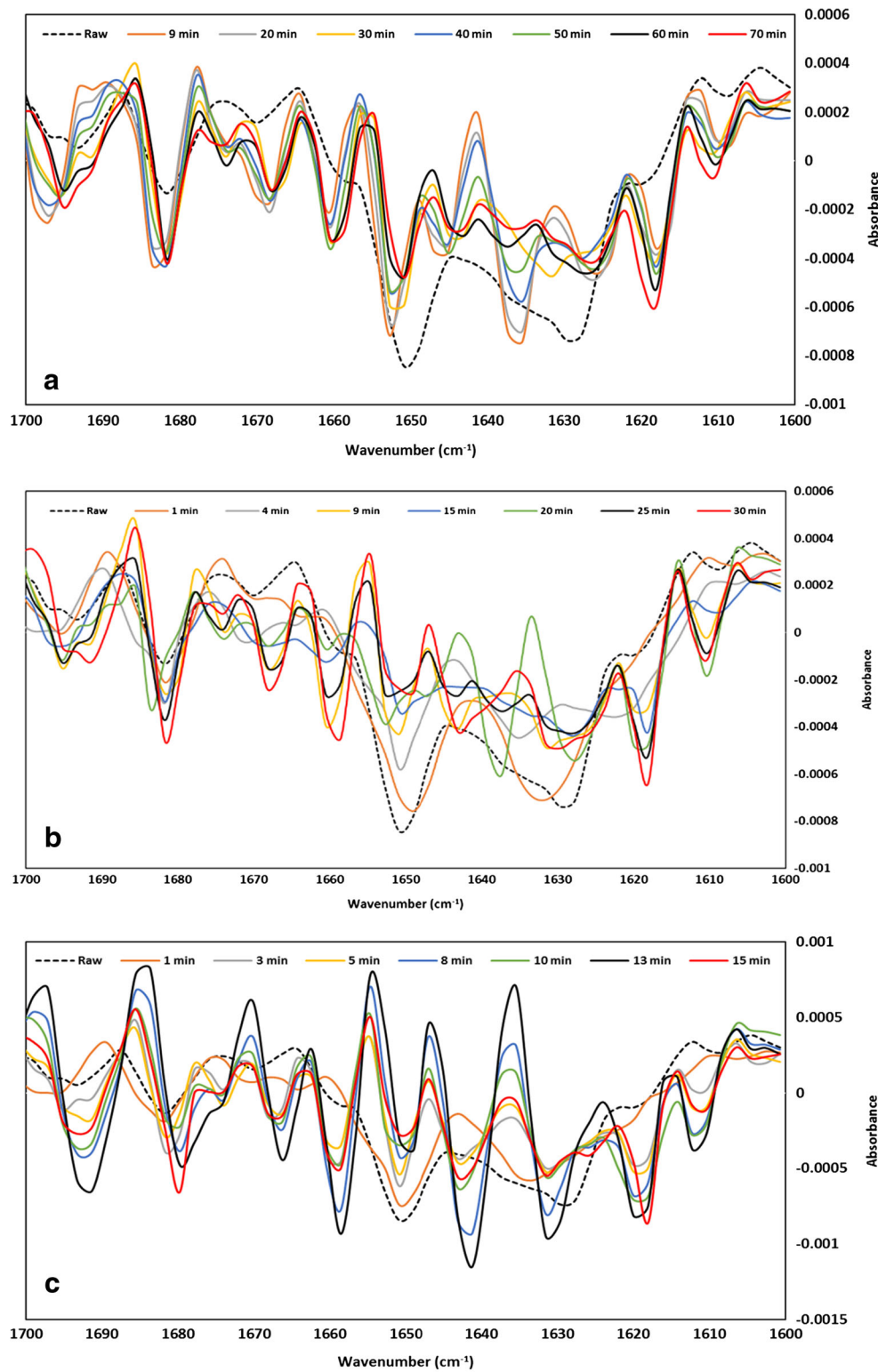


Fig. 4 Second derivative of the amide I band ($1700\text{--}1600\text{ cm}^{-1}$) in raw and thermally processed Atlantic salmon muscle at different temperatures. **a** $55\text{ }^{\circ}\text{C}$. **b** $65\text{ }^{\circ}\text{C}$. **c** $75\text{ }^{\circ}\text{C}$. **d** $85\text{ }^{\circ}\text{C}$. **e** $90\text{ }^{\circ}\text{C}$

heating time and temperature increased from 0.534 in raw samples to 0.375 in samples heated at $90\text{ }^{\circ}\text{C}$ for 14 min ($P < 0.05$). To enhance the spectra in the amide I region, second derivative

spectra were provided. Second derivative spectra showed the bands at 1695, 1682, 1668, 1660, 1651, 1631, 1625, 1618, and 1611 cm^{-1} (Fig. 4a–e), as anticipated for raw Atlantic

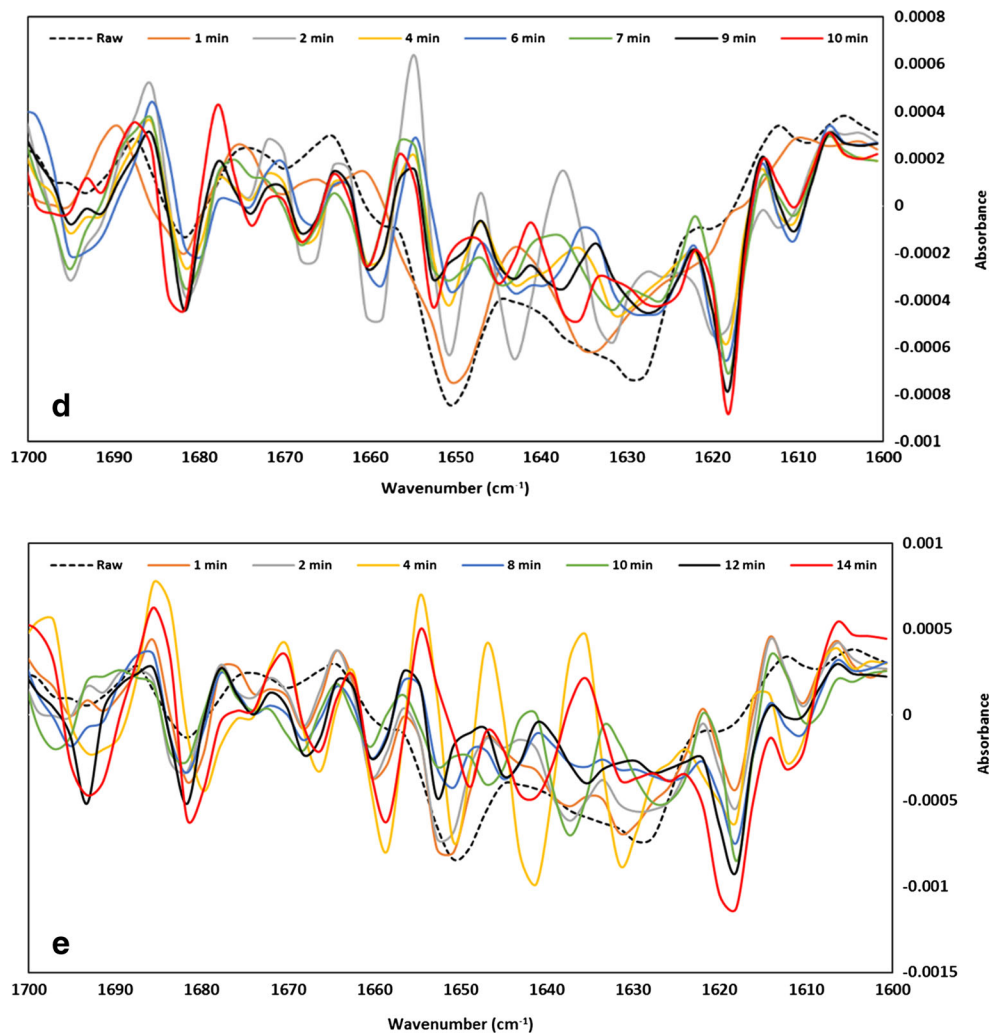


Fig. 4 continued.

salmon (Bocker et al. 2008; Ojagh et al. 2011). The band at 1652 cm^{-1} was assigned to the α -helical structures, which are present in 90% of the myosin protein and are related to loop structures (Kirschner et al. 2004; Bertram et al. 2006; Bocker et al. 2008). The highest intensity for this peak occurred in raw samples; however, increasing the heating time and temperature decreased the intensity significantly ($P < 0.05$). This indicates that protein denaturation and unfolding increased by increasing the heating time and temperature. Other researchers found that increasing the temperature decreases the intensity of this peak (Wu et al. 2006; Ojagh et al. 2011). The intensity of the peak at 1618 cm^{-1} increased significantly ($P < 0.05$) as time and temperature increased. This is attributed to the β -sheet structures, indicating increased aggregation in cooked samples at the intermolecular level (Carton et al. 2009; Ojagh et al. 2011). The same trend was observed at 1682 cm^{-1} , which is related to changes in intramolecular antiparallel β -sheet structures in heated samples. This accords with previous findings (Carton et al. 2009; Ojagh et al. 2011). Generally, the bands below 1640 cm^{-1} are assigned

to the β -sheet structure changes, indicating protein aggregation (Carton et al. 2009). Results demonstrate the effects of heating on muscle protein. This can be detected from α -helical structures changes or both intramolecular and intermolecular aggregation of the β -sheet by decreasing the intensity at 1651 cm^{-1} and increasing the intensity at 1695 , 1682 , 1625 , and 1618 cm^{-1} compared to the raw samples.

Principal component analysis (PCA) was applied to study the variance of the myofiber spectra for heated Atlantic salmon at different times and temperatures. PCA results for different temperatures are presented in Fig. 5a–e. For $55\text{ }^{\circ}\text{C}$, nearly 64% of the variance is explained by PC1 and 27% is explained by PC2, at 65 , 75 , 85 , and $90\text{ }^{\circ}\text{C}$. PC1 and PC2 explained 83 and 11%, 85 and 10%, 90 and 5%, and 76 and 12% of the variance, respectively.

Correlation loading plot results indicate that at lower temperatures (55 to $75\text{ }^{\circ}\text{C}$), PC1 is related to protein denaturation (1660 to 1651 cm^{-1}), while PC2 is dominated by β -sheet aggregation (1695 and 1618 cm^{-1}). However, at 85 and

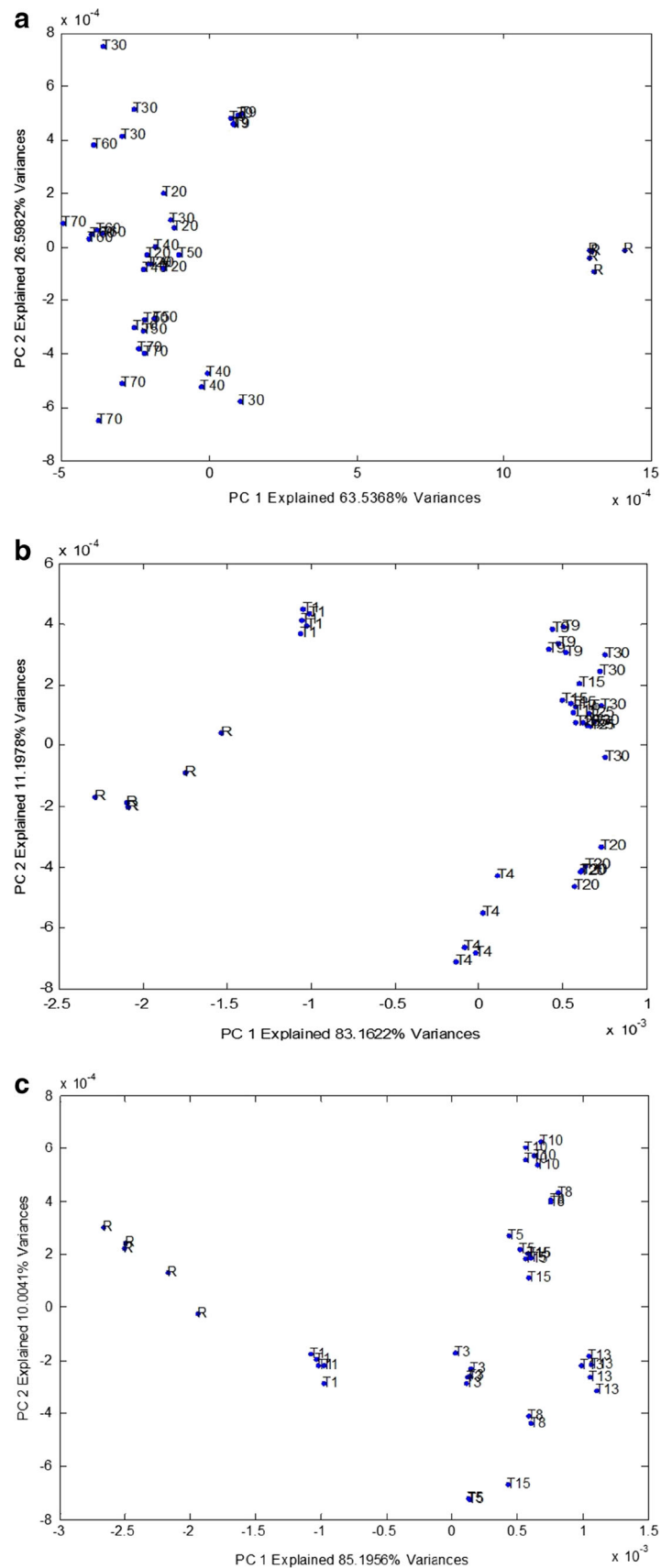


Fig. 5 Principal component analysis (PCA) of raw and thermally processed Atlantic salmon muscle at different temperatures. **a** 55 °C. **b** 65 °C. **c** 75 °C. **d** 85 °C. **e** 90 °C

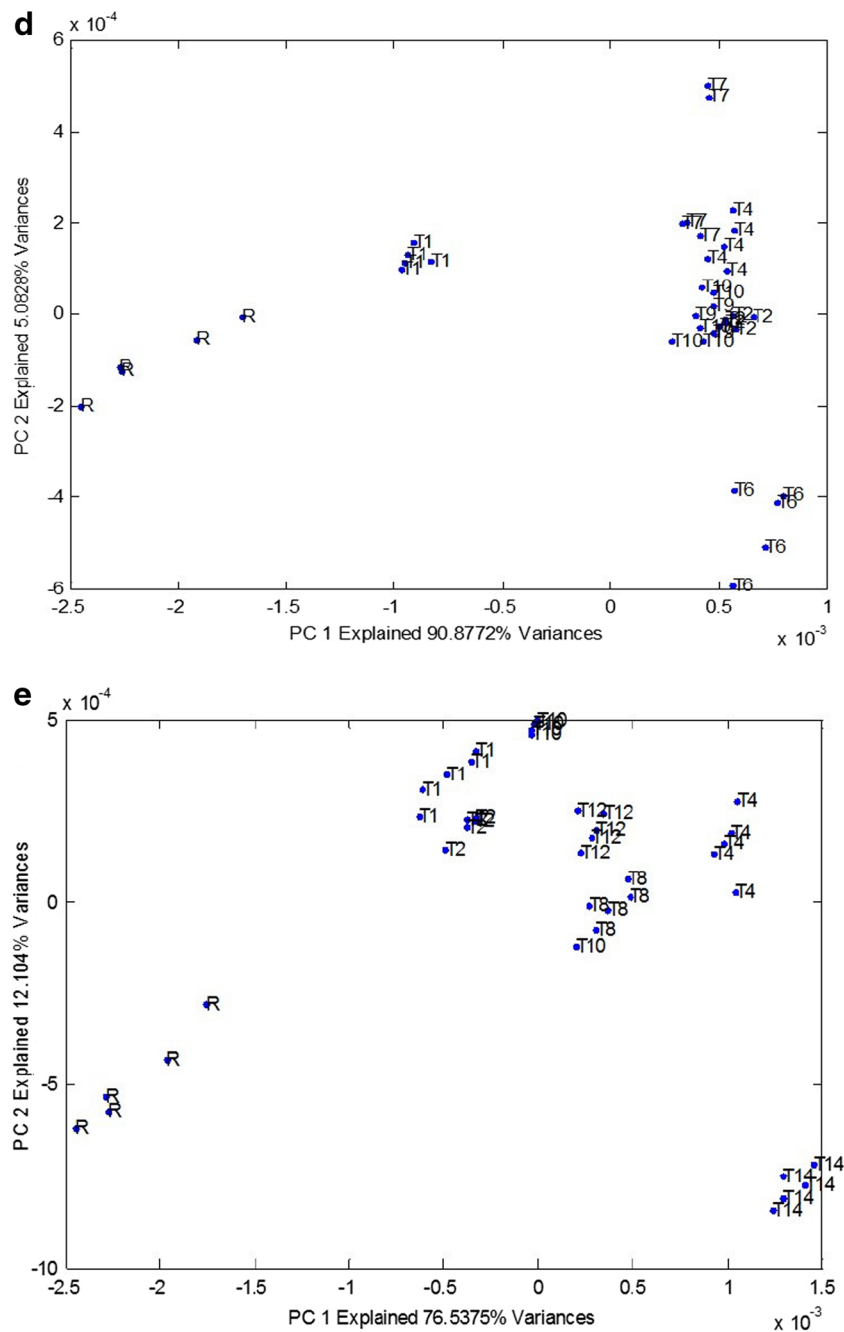


Fig. 5 continued.

90 °C, PC1 and PC2 both are related to protein aggregation due to a large increase in peak intensity at 1618 and 1695 cm^{-1} . These results show that at lower temperatures, protein denaturation and unfolding of α -helix are dominant and at higher temperatures protein aggregation of β -sheet is more superior in protein degradation. At higher temperatures, the protein denaturation rate is faster than protein aggregation. This accords with our findings using DSC and dielectric properties. Carton et al. (2009) studied the protein denaturation of Atlantic salmon during salting and

smoking using FTIR. They found that by increasing the salting time, protein aggregation in the β -sheet becomes dominant, while α -helix denaturation played a lesser role. Bocker et al. (2008) subject Atlantic salmon muscle samples to different salt concentrations. They found that α -helical structures were higher in samples with lower salt concentrations due to less protein unfolding and denaturation. Yan et al. (2004) studied heat-induced unfolding and aggregation of hemoglobin and found that at lower temperature (46 to 60 °C), changes in protein are dominated by α -helical structures. At higher

temperatures, this is mainly determined by β -sheet structural changes.

Hence, results demonstrate that 75 °C is the transition or critical temperature for Atlantic salmon muscle protein during thermal processing. Our DSC and dielectric property studies also produced the same results.

DSC Protein Denaturation

Figure 6a–c displays the contour plot graphs for different proteins (myosin, sarcoplasmic proteins, and actin) and denaturation temperatures. Results indicate that myosin and sarcoplasmic proteins completely denatured after 20 min at 55 °C, after 4 min at 65 °C, and after 1 min at 75 °C and were not detectable at 85 and 90 °C. This demonstrates that the protein denaturation rate increases as temperature increases. At higher temperatures, the protein denaturation rate was faster than the protein aggregation. This accords with our findings for dielectric properties and FTIR. DSC is often used to determine the temperature of protein denaturation in many seafoods, including cod (*G. morhua*) (Ofstad et al. 1996), Atlantic salmon (*S. salar*) and scallops (*Chlamys tehuelchus*) (Paredi et al. 1998), Atlantic cod (*G. morhua*) (Skipnes et al. 2008), Pacific white shrimp (*Litopenaeus vannamei*) (Rattanasatheirn et al. 2008), Southern Ocean swimming crab (*Ovalipes trimaculatus*) and Patagonian stone crab (*Platyxanthus patagonicus*) (Dima et al. 2012), black tiger shrimp (*Penaeus monodon*) (Jantakoson et al. 2012), and brown shrimp (*Crangon crangon*) (Verhaeghe et al. 2016). However, there are no systematic studies to determine the effects of heating time and temperature on protein denaturation in precooked salmon. Denaturation enthalpy, ΔH , is a net value of endothermic and exothermic reactions that are related to intact protein (Ma and Harwalkar 1991). In this study, we observed four peaks in raw Atlantic salmon and found that the temperatures of protein denaturation were 43 °C, 56–58 °C for myosin and collagen, 65–67 °C for sarcoplasmic proteins, and 76–78 °C for actin. This accords with results found by Ofstad et al. (1996) for a raw Atlantic salmon DSC thermogram. Skipnes et al. (2008) observed five peaks in cod muscle and assigned the first peak to myosin because there is less collagen in fish muscle. They also proposed that the decrease in residual enthalpy and smaller peaks at higher temperatures corresponded to the unfolding of cod muscle proteins.

Our results show a decrease in enthalpy and in the myosin and sarcoplasmic proteins at 65 to 75 °C. This accords with our FTIR and dielectric loss factor kinetic results, in which 75 °C was the critical temperature. Above this temperature, the protein denaturation rate was faster than that of protein aggregation. Our results also indicate that actin is the most heat-resistant protein, so that its residual enthalpy can be used in the kinetic study of protein denaturation (Skipnes et al. 2008; Verhaeghe et al. 2016).

Dielectric Properties

Many researchers have examined the dielectric properties of food proteins (Guan et al. 2004; Brunton et al. 2006; Basaran et al. 2010, Wang et al. 2003; Wang et al. 2008; Wang et al. 2009). However, most measured dielectric properties at different temperatures using the real-time method in raw foods. Their aim was to develop thermal processing of foods using radio and microwave frequencies as a function of food composition, temperature, and the frequencies. In this study, we measured the dielectric properties of precooked Atlantic salmon muscle at 22 °C to study the protein denaturation. We measured the dielectric properties (ϵ' and ϵ'') of raw and precooked Atlantic salmon at 27, 40, 915, and 1800 MHz at room temperature. The dielectric constant and loss for the raw sample were 50 ± 5.8 and 224.2 ± 0.2 , at 27 MHz, respectively, and 46.1 ± 5.6 and 154 ± 0.4 , at 40 MHz, respectively. Results showed that increasing the time and temperature of thermal processing significantly increases the dielectric constant and dielectric loss ($P < 0.05$) at lower frequencies (27 and 40 MHz) (Table 4). At higher frequencies (915 and 1800 MHz) (data not shown), there was little change. This may be due to less ionic conductivity and dipole loss component at higher frequencies (Brunton et al. 2006; Wang et al. 2008). Other researchers also reported better protein denaturation detection at radiofrequencies compared to microwave frequencies (Guan et al. 2004; Brunton et al. 2006; Basaran et al. 2010, Wang et al. 2003; Wang et al. 2008; Wang et al. 2009). During protein denaturation, calcium and magnesium ions are released, and since dielectric loss is more dependent upon ionic mobility at low frequencies, greater changes were observed at 27 and 40 MHz (Brunton et al. 2006).

Both the dielectric constant and dielectric loss increased at 27 and 40 MHz, indicating that protein degradation occurred during thermal processing. However, due to more sensitivity of dielectric loss, it showed larger increase compared to dielectric constant (Ahmed et al. 2008; Wang et al. 2003; Wang et al. 2008; Wang et al. 2009). Dielectric loss is associated with mobility, while the dielectric constant is not sensitive to mobility associated with protein denaturation, and is a measure of the molecular dipole. Thus, the dielectric constant may not show significant change associated with the protein structure (Barringer et al. 1995). In our study, the dielectric properties were lower than that of Atlantic salmon, as reported by Basaran et al. (2010). This might be due to different measurement strategies and methods. Basaran et al. (2010) measured the dielectric properties of the samples using the real-time method, while we measured the dielectric properties of the precooked samples at 22 °C. Since dielectric properties are related to the state of the water in foods, and since the mobility of water increases when it is heated, the dielectric properties were higher during heating. However, in precooked samples, water molecules have less mobility and exhibit less change in

Fig. 6 Contour plot of enthalpy changes for different proteins. **a** Myosin. **b** Sarcoplasmic proteins. **c** Actin

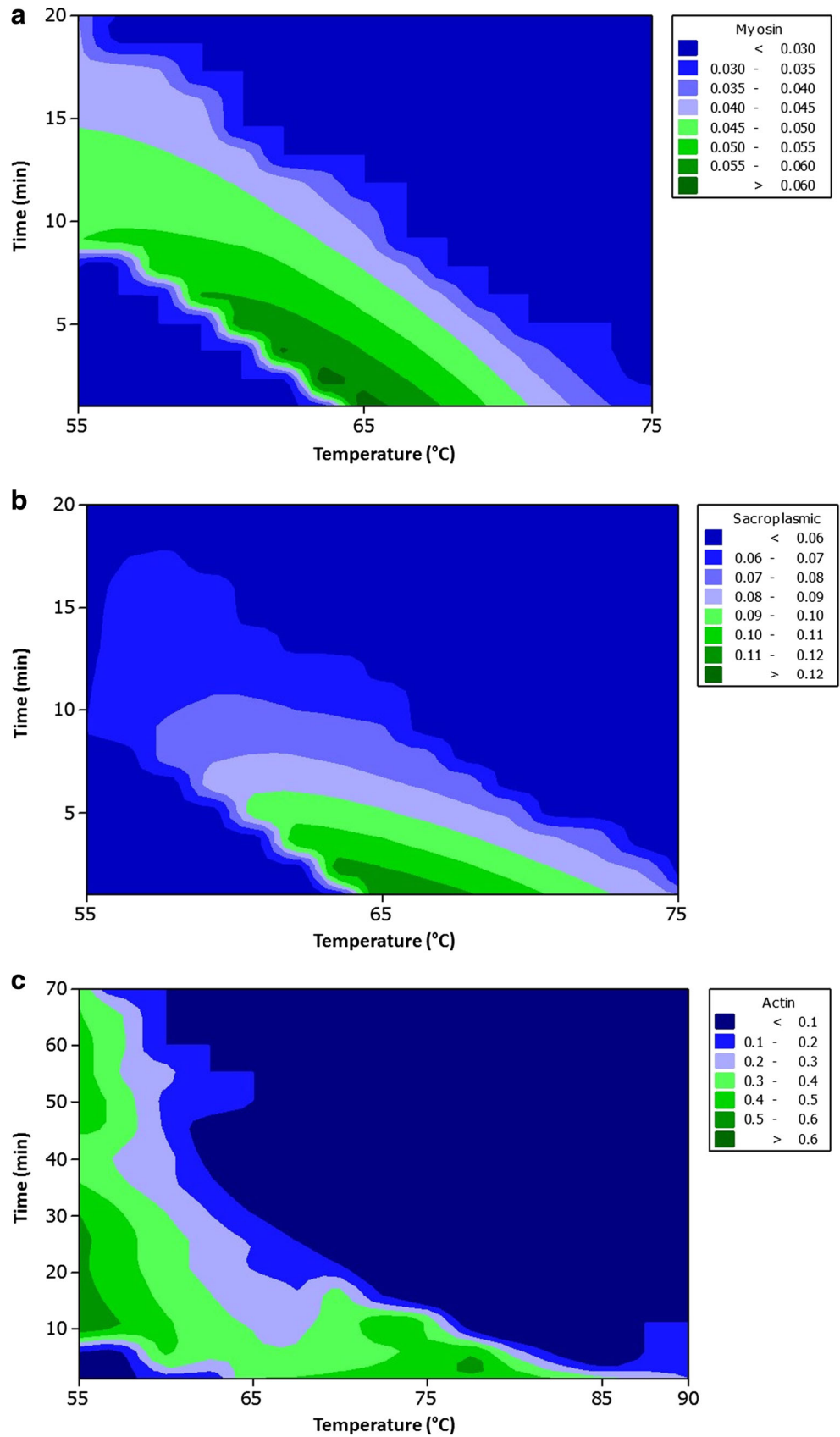


Table 4 Dielectric properties (ϵ' and ϵ'') and penetration depth of precooked Atlantic salmon at RF frequencies

T (°C)	Time (min)	27 MHz			40 MHz		
		ϵ'	ϵ''	Dp (mm)	ϵ'	ϵ''	Dp (mm)
55	9	87.2 ± 5.2	398.1 ± 16.5	68.4 ± 1.5	78.6 ± 4.1	270.8 ± 15.9	58.1 ± 2.5
	20	87.8 ± 6.1	459.9 ± 24.3	62.8 ± 1.1	79.1 ± 3.5	285.1 ± 18.1	56.2 ± 3.1
	30	88.7 ± 4.3	468.4 ± 28.1	62.1 ± 0.6	80.1 ± 2.7	302.8 ± 27.4	54.2 ± 2.8
	40	89.8 ± 2.8	475.4 ± 22.5	61.7 ± 1.7	80.2 ± 2.5	320.7 ± 17.3	52.3 ± 1.7
	50	95.5 ± 3.6	483.2 ± 43.1	61.4 ± 3.2	85.6 ± 1.8	328.4 ± 31.6	52.1 ± 1.4
	60	96.1 ± 5.3	498.8 ± 46.7	60.3 ± 3.6	85.7 ± 1.3	341.8 ± 28.5	50.7 ± 1.8
	70	96.7 ± 5.8	509.5 ± 43.1	59.6 ± 2.4	87 ± 2.1	350.8 ± 22.1	50 ± 3.4
	1	70.8 ± 4.4	338.8 ± 30.4	73.8 ± 1.2	64 ± 2.4	236.1 ± 19.2	61.6 ± 3.2
65	4	76 ± 5.1	453.1 ± 30.8	62.5 ± 1.3	68.8 ± 1.4	240.9 ± 21.9	61.4 ± 1.6
	9	88.6 ± 5.5	481.1 ± 38.5	61.1 ± 3.2	80.1 ± 2.2	275.4 ± 17.1	57.6 ± 2.4
	15	89.3 ± 4.7	492.8 ± 22.4	60.3 ± 2.3	83.5 ± 3.7	298.1 ± 18.3	55.1 ± 3.2
	20	91.4 ± 2.8	519.1 ± 31.4	58.6 ± 0.8	84.2 ± 3.3	319.3 ± 21.1	52.7 ± 3.1
	25	95.7 ± 6.1	521.9 ± 43.1	58.7 ± 1.7	85.9 ± 2.1	324.1 ± 32.7	52.4 ± 2.8
	30	96.2 ± 4.2	528.1 ± 20.4	58.3 ± 0.7	86.3 ± 1.4	342.43 ± 27.8	50.7 ± 1.5
	1	77.6 ± 1.8	386.3 ± 18.3	68.8 ± 0.5	67.9 ± 3.2	268.3 ± 27.3	57.3 ± 3.2
	3	92.6 ± 4.3	457.4 ± 23.4	63.3 ± 0.9	83.4 ± 1.1	315.1 ± 18.4	53.2 ± 0.6
75	5	95.7 ± 1.2	467.1 ± 21.4	62.7 ± 1.3	84.4 ± 4.1	345.9 ± 30.4	50.2 ± 2.1
	8	96.2 ± 3.3	479.2 ± 31.5	61.8 ± 1.4	84.9 ± 3.4	352.3 ± 24.3	49.7 ± 3.5
	10	97.4 ± 4.1	488.1 ± 28.1	61.2 ± 1.8	85.1 ± 2.4	362.7 ± 28.5	48.85 ± 2.1
	13	97.2 ± 2.8	495.1 ± 33.5	60.6 ± 1.4	85.7 ± 2.5	387.7 ± 29.4	47.1 ± 2.6
	15	97.7 ± 1.9	512.5 ± 18.4	59.4 ± 0.4	85.4 ± 1.8	408.7 ± 19.3	45.4 ± 1.1
	1	95 ± 2.1	418.3 ± 26.5	66.9 ± 0.6	86.4 ± 1.6	312.7 ± 33.5	53.7 ± 1.3
	2	95.1 ± 3.1	449.1 ± 38.1	64.1 ± 2.1	86.9 ± 2.1	339.8 ± 25.8	50.9 ± 2.4
	4	96.5 ± 2.6	451.8 ± 27.4	64.1 ± 1.5	87.2 ± 2.4	361.3 ± 23.5	49.1 ± 2.3
85	6	97 ± 1.7	464.8 ± 22.7	62.9 ± 0.7	87.5 ± 1.8	373.6 ± 18.6	48.1 ± 0.5
	7	97.7 ± 4.3	478.3 ± 41.5	61.9 ± 2.1	87.8 ± 3.1	384.3 ± 21.7	47.3 ± 2.3
	9	98.2 ± 2.2	496.8 ± 25.7	60.6 ± 1.6	89.4 ± 3.2	412.1 ± 25.3	45.4 ± 3.5
	10	100.5 ± 3.2	532.5 ± 28.3	58.2 ± 2.1	89.9 ± 1.5	431.8 ± 23.4	44.2 ± 1.6
	1	97 ± 3.4	425.4 ± 31.2	66.4 ± 3.2	86.4 ± 1.1	294.6 ± 18.4	55.7 ± 0.9
	2	98.3 ± 2.6	494.1 ± 34.8	60.7 ± 2.6	87.1 ± 2.5	323.9 ± 19.5	52.5 ± 1.6
	4	101.8 ± 1.5	545.1 ± 28.7	57.5 ± 1.2	87.7 ± 3.1	366.3 ± 30.4	48.7 ± 3.5
	8	103 ± 2.1	597.2 ± 41.2	54.5 ± 1.5	89.1 ± 3.7	389.6 ± 22.4	46.9 ± 3.6
90	10	106.8 ± 3.4	608.7 ± 44.5	54.1 ± 3.1	91.5 ± 2.1	448.3 ± 21.7	43.3 ± 2.4
	12	109.5 ± 1.8	628.1 ± 38.2	53.2 ± 2.4	93.7 ± 1.4	470.8 ± 25.4	42.1 ± 1.3
	14	109.6 ± 1.4	639.2 ± 27.5	52.7 ± 1.5	94.1 ± 2.7	488.4 ± 25.8	41.2 ± 1.5

dielectric properties (Wang et al. 2003; Wang et al. 2009). Another possibility is that there is less moisture content due to cook loss in precooked samples (Wang et al. 2003). Wang et al. (2009) measured the dielectric properties of liquid and precooked egg protein and found that dielectric properties were lower in precooked egg protein compared with liquid egg protein.

Protein degradation starts with unfolding the protein molecules due to heat, exposing the interior hydrophobic, non-polar regions, and sulfhydryl groups. This process continues by

aggregation, due to intermolecular interactions (Clark 1998). After protein degradation, the majority of fluid is expelled from the molecules. Due to cook loss, the protein molecules shrink and their mobility tends to increase. Since the dielectric properties are related to the mobility of water and ions, an increase in mobility in the fluid causes an increase in dielectric properties (Bircan and Barringer 2002; Ahmed et al. 2008). Therefore, it is clear that protein denaturation and aggregation have the most critical impact on the dielectric properties of muscle foods. Basaran et al. (2010) applied the microbial

transglutaminase (MTGase) enzyme to improve protein functionality in chicken and fish muscle. They found that samples with MTGase showed higher dielectric properties due to the aggregation of proteins from MTGase polymerization. We also examined the secondary structure of protein using FTIR. Results show a decrease in α -helix (protein denaturation) and an increase in β -sheet (protein aggregation), which were less at lower temperatures than at higher temperatures, and changed with increasing time and temperature of pasteurization. FTIR results at the intramolecular and intermolecular levels accord with our findings on changes in dielectric properties changes during thermal processing. In fact, dielectric properties were lower in samples that were thermally treated at lower temperatures. For example, at 55 °C, the maximum dielectric constant and dielectric loss were 96.7 and 509 at 27 MHz, respectively, and 87 and 350 at 40 MHz, respectively, after 70 min. However, at 90 °C, after 1 min, the dielectric constant and dielectric loss were 97 and 425.4 at 27 MHz and 86.1 and 294.6 at 40 MHz, respectively. One explanation is the denaturation temperature of different types of proteins varies. The temperature of protein denaturation in salmon muscle was 43 and 56–58 °C for myosin, 65–67 °C for sarcoplasmic proteins, and 76–78 °C for actin, according to our DSC thermogram. Our DSC results showed that, at 55 °C, myosin and sarcoplasmic proteins completely denatured after 20 min heating. However, actin, the most heat-resistant protein, was not denatured at lower temperature. By increasing the temperature to 75 °C, myosin and sarcoplasmic proteins denatured within 1 min of heating, and the actin peak was not detectable after 30 min. At 85 and 90 °C, myosin and sarcoplasmic proteins peaks were not detectable, and actin was completely denatured after 4 and 2 min at 85 and 90 °C, respectively (Fig. 6). Hence, based on FTIR and DSC results, more protein aggregation occurred at higher

temperatures, leading to a higher dielectric constant and dielectric loss at higher temperatures.

The penetration depth decreased significantly as heating time and temperature increased, indicating that as changes in the protein structure increased compared to the native protein, the penetration depth decreased. The penetration depth for raw samples was 97.3 and 77.2 mm at 27 and 40 MHz, respectively. The penetration depth for all samples was higher at 27 MHz compared to 40 MHz and decreased as the temperature and protein denaturation increased. This is in accord with prior findings (Ahmed et al. 2008; Wang et al. 2003; Wang et al. 2008; Basaran et al. 2010).

Kinetics of Protein Degradation

Since dielectric loss was highly temperature-dependent, this parameter was used to calculate the kinetics of protein degradation over a range of 27 and 40 MHz. Many researchers have examined protein denaturation and aggregation kinetics in foods using DSC or HPLC. Both methods directly measure the protein denaturation rate, which is related to the unfolding of protein in response to temperature. However, in this study, we used both DSC and dielectric loss to measure the kinetics of protein denaturation. DSC provides a direct measurement of protein denaturation due to enthalpy changes in the thermogram. Dielectric loss provides indirect measurement of protein denaturation by measuring the mobility of the water as a result of protein denaturation. Results on dielectric loss indicate that protein degradation followed a first-order reaction. Figure 7 shows the temperature dependency of protein degradation during thermal processing. Clearly, the denaturation rate increases with temperature. This accords with prior findings on protein denaturation in response to heat (Wolz and Kulozik 2015). The Arrhenius model

Fig. 7 Temperature dependence of protein denaturation rate, measured as dielectric loss at 27 and 40 MHz

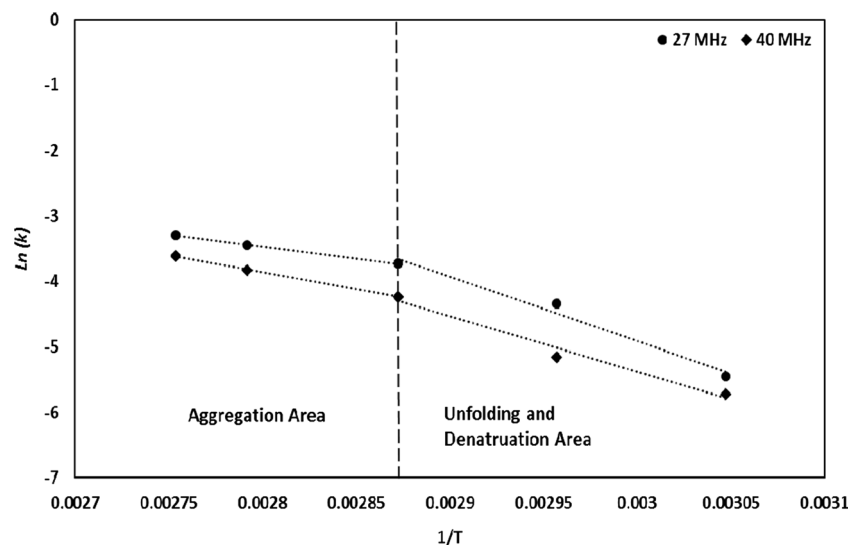


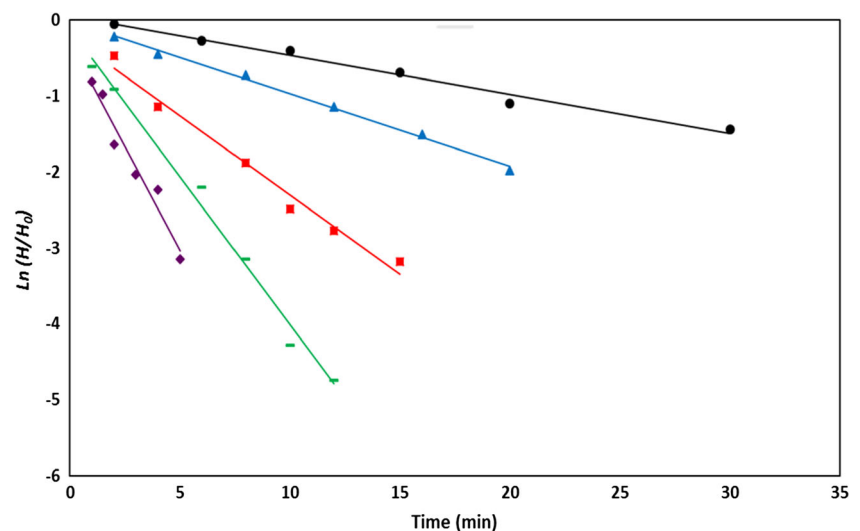
Table 5 First-order kinetic parameters for protein degradation of Atlantic salmon after heat treatment at different temperatures (68–74 °C)

Reaction area	E_a (kJ/mol)	k_0 (min ⁻¹)	R^2
Unfolding	339.1	6.5×10^{47}	0.9950
Aggregation	238.9	4.1×10^{32}	0.9735
Total	300.6	1.1×10^{42}	0.9864

(Fig. 7) for the dielectric loss factor at 27 and 40 MHz showed a two-step reaction. This included unfolding and the protein denaturation step at low temperatures, along with the aggregation step at higher temperatures, separated by the critical temperature at 75 °C. The critical temperature separates the Arrhenius plot into two sections. At temperatures above the critical temperature (75 °C), unfolding and protein denaturation take place faster than aggregation, which is in agreement with our FTIR and DSC results. The FTIR correlation loading plot results show that at lower temperatures (55 to 75 °C), the PC1 is related to protein denaturation (1660 to 1651 cm⁻¹) and PC2 is dominated by β -sheet aggregation (1695 and 1618 cm⁻¹). However, at 85 and 90 °C, PC1 and PC2 both are related to protein aggregation due to the strong increasing in peak intensity at 1618 and 1695 cm⁻¹. In addition, DSC results show that at above 75 °C, only the actin peak could be detected within 4 and 2 min, for 85 and 90 °C, respectively. In addition, most of the proteins has been already denatured. Other researchers report the same trend for the heated whey protein, with a critical temperature of 80 °C (Khaldi et al. 2015; Wolz and Kulozik 2015). In our study, the activation energy for the unfolding step at 27 and 40 MHz was 82.1 and 70.1 kJ/mol, respectively, which was lower than prior findings. The DSC protein degradation kinetics at 68 to 74 °C showed that the activation energies for unfolding and the aggregation area were 339.1 and 238.9 kJ/mol, respectively. The total protein degradation activation energy was 300.6 kJ/mol (Table 5),

which is in the range of protein denaturation activation energies reported by other researchers. Activation energies for some proteins were 172 and 176 kJ/mol for Pacific Whiting and Alaska Pollock surimi, respectively, at 80% moisture content (Yoon et al. 2004), 342 kJ/mol at the concentration of 10% for whey protein (Wolz and Kulozik 2015), 388 kJ/mol for shrimp protein (Verhaeghe et al. 2016), 384 kJ/mol for whey protein (Khaldi et al. 2015), and 145 and 156 kJ/mol for Patagonian marine crabs, respectively (Dima et al. 2012). Wolz and Kulozik (2015) reported that the activation energy for aggregation (126 kJ/mol) is significantly lower than unfolding (342 kJ/mol) in whey protein at 10% concentration. This may be due to the high impact of temperature on unfolding compared to aggregation (Wolz and Kulozik 2015).

The difference between the activation energy results from dielectric properties from this study, and the DSC could be explained by two major facts, including the difference between the protein degradation measurement methods, which in current study the dielectric loss which is an indirect method for measuring the protein structure was applied, while DSC can provide the direct measurement of protein denaturation. Temperature range can also affect activation energy. In the dielectric study, we measured all protein degradation in the temperature range of 55 to 90 °C. However, in the DSC study, we applied only temperatures within 10 °C range and only examined actin denaturation enthalpy. Results from our DSC study at 66 to 74 °C were in agreement with other researchers. Our DSC results indicate that protein denaturation followed a first-order reaction, similar to other researchers' reports (Grinberg et al. 2000; Skipnes et al. 2008; Dima et al. 2012; Mao et al. 2016; Verhaeghe et al. 2016). Figure 8 shows the thermal denaturation of actin protein measured by DSC as a function of time at different temperatures from 66 to 74 °C. The curve slope indicating the protein denaturation rate increased with temperature. This indicates the high temperature

Fig. 8 Residual denaturation enthalpy of Atlantic salmon precooked muscle at 66 °C (black circle), 68 °C (black up-pointing triangle), 70 °C (black square), 72 °C (en dash), and 74 °C (black diamond) as a function of treatment time

dependence of actin protein denaturation, according with results of other researchers, who measured the protein denaturation rate for a small range of temperatures (Skipnes et al. 2008; Verhaeghe et al. 2016).

Conclusions

This study was aimed to determine the kinetics of quality degradation and protein denaturation and aggregation using different methods to provide valuable information for optimizing the thermal processing of Atlantic salmon. We found that cook loss and area shrinkage were increased as the time and temperature of heating increased, and kinetic models were fitted to a first-order reaction. By increasing the heating time and temperature, the color of the Atlantic salmon muscle increased opacity and the *L* value by a zero-order reaction. We found that FTIR spectra in the amide I region could be used to investigate protein denaturation (α -helix) and protein aggregation (β -sheet). FTIR spectra chemometrics of the secondary structure of protein revealed that by increasing the temperature and time, the peak intensity of the α -helix decreased, while the peak intensity of β -sheet increased significantly. We also found that the protein denaturation rate was higher above the transition temperature (75 °C). Dielectric properties indicate that by increasing time and temperature, protein denaturation and aggregation increased significantly and dielectric properties may be used to measure protein denaturation. Findings from our kinetic study of protein denaturation using DSC suggest the first-order model for protein denaturation with 300.6 kJ/mol activation energy. Findings from this study can provide rapid detection methods and mathematical models to predict and study protein degradation and improve thermal processing. By combining several models in this study with microbial inactivation kinetic, they can be applied to identify optimum processing conditions, including time and temperature, to enhance the safety and quality of Atlantic salmon RTE products.

Acknowledgements This study was partially funded by the following grants: USDA-NIFA 2011-68003-20096, USDA-NIFA 2016-68003-24840, as well as the Agricultural Research Center at Washington State University. The authors would like to thank Dr. Setareh Shiroodi at UC Davis, California; Dr. Kanishka Bhunia, Dr. Huimin Lin, Mr. Frank Loring Younce, and Mr. Stewart Bohnet at Washington State University, Pullman, Washington; and Dr. Xiaonan Lu and Ms. Yaxi Hu at the University of British Columbia, Vancouver, Canada for technical support.

References

Ahmed, J., Ramaswamy, H. S., & Raghavan, G. S. V. (2008). Dielectric properties of soybean protein isolate dispersions as a function of concentration, temperature and pH. *LWT-Food Science and Technology*, *41*, 71–81.

- Astruc, T., Peyrin, F., Venien, A., Labas, R., Abrantes, M., Dumas, P., & Jamme, F. (2012). In situ thermal denaturation of myofibre sub-type proteins studied by immunohistofluorescence and synchrotron radiation FT-IR microspectroscopy. *Food Chemistry*, *134*, 1044–1051.
- Basaran, P., Basaran-Akgul, N., & Rasco, B. (2010). Dielectric properties of chicken and fish muscle treated with microbial transglutaminase. *Food Chemistry*, *120*, 361–370.
- Barbera, S., & Tassone, S. (2006). Meat cooking shrinkage: measurement of a new meat quality parameter. *Meat Science*, *73*(3), 467–474.
- Barringer, S. A., Fleischmann, A. M., Davis, E. A., & Gordon, J. (1995). The dielectric properties of whey protein as indicators of change in polymer mobility. *Food Hydrocolloids*, *9*, 343–348.
- Bertola, N. C., Bevilacqua, A. E., & Zaritzky, N. E. (1994). Heat treatment effect on texture changes and thermal denaturation of proteins in beef muscle. *Journal of Food Processing and Preservation*, *18*, 31–46.
- Bertram, H. C., Kohler, A., Bocker, U., Ofstad, R., & Andersen, H. J. (2006). Heat-induced changes in myofibrillar protein structure and myowater of two pork qualities. A combined FT-IR spectroscopy and low-field NMR relaxometry study. *Journal of Agricultural and Food Chemistry*, *54*, 1740–1746.
- Bhattacharya, S., Choudhury, G. S., & Studebaker, S. (1994). Color changes during thermal processing of Pacific chum salmon. *Journal of Aquatic Food Product Technology*, *3*(1), 39–48.
- Bircan, C., & Barringer, S. A. (2002). Use of dielectric properties to detect egg protein denaturation. *Journal of Microwave Power and Electromagnetic Energy*, *37*, 90–96.
- Bocker, U., Kohler, A., Aursand, I. G., & Ofstad, R. (2008). Effects of brine salting with regards to raw material variation of Atlantic salmon (*Salmo salar*) muscle investigated by Fourier transform infrared microspectroscopy. *Journal of Agricultural and Food Chemistry*, *56*, 5129–5137.
- Brunton, N. P., Lyng, J. G., Zhang, L., & Jacquier, J. C. (2006). The use of dielectric properties and other physical analyses for assessing protein denaturation in beef *Biceps femoris* muscle during cooking from 5 to 85°C. *Meat Science*, *72*, 236–244.
- Buffler, C. R. (Ed.). (1993). *Microwave cooking and processing* (pp. 47–68). New York: Van Nostrand Reinhold.
- Cao, L., Rasco, B., Tang, J., Niu, L., Lai, K., Fan, Y., & Huang, Y. (2016). Effects of freshness on the cool loss and shrinkage of grass carp (*Ctenopharyngodon idellus*) fillets following pasteurization. *International Journal of Food Properties*, *19*, 2297–2306.
- Carton, I., Bocker, U., Ofstad, R., Sorheim, O., & Kohler, A. (2009). Monitoring secondary structural changes in salted and smoked salmon muscle myofiber proteins by FT-IR microspectroscopy. *Journal of Agricultural and Food Chemistry*, *57*, 3563–3570.
- Clark, A. H. (1998). Gelation of globular proteins. In S. E. Hill, D. A. Ledward, & J. R. Mitchell (Eds.), *Functional properties of food macromolecules* (2nd ed., pp. 77–142). Gaithersburg: Aspen Publisher.
- Dima, J. B., Barón, P. J., & Zaritzky, N. E. (2012). Mechanical modeling of the heat transfer process and protein denaturation during the thermal treatment of Patagonian marine crabs. *Journal of Food Engineering*, *113*, 623–634.
- FAO (2014). Atlantic salmon production statistics. <http://www.fao.org/fishery/species/2929/en>.
- Gaze, J. E., Boyd, A. R., & Shaw, H. L. (2006). Heat inactivation of *Listeria monocytogenes* Scott A on potato surfaces. *Journal of Food Engineering*, *76*, 27–31.
- Gibson, K. E., & Schwab, K. J. (2011). Thermal inactivation of human norovirus surrogates. *Food and Environmental Virology*, *3*, 74–77.
- Grinberg, V. Y., Burova, T. V., Haertl, T., & Tolstoguzov, V. B. (2000). Interpretation of DSC data on protein denaturation complicated by kinetic and irreversible effects. *Journal of Biotechnology*, *79*, 269–280.

- Guan, D., Cheng, M., Wang, Y., & Tang, J. (2004). Dielectric properties of mashed potatoes relevant to microwave and radio-frequency pasteurization and sterilization processes. *Journal of Food Science*, 69(1), 30–37.
- Haard, N. F. (1992). Biochemistry and chemistry of color and color changes in seafoods. In G. J. Flick & R. E. Martin (Eds.), *Advances in seafood biochemistry: composition and quality* (pp. 305–360). Lancaster, PA: Technomic Publishing Company Inc..
- Jantakoson, T., Kijroongrojana, K., & Benjakul, S. (2012). Effect of high pressure and heat treatments on black tiger shrimp (*Penaeus monodon* Fabricius) muscle protein. *International Aquatic Research*, 4, 19. doi:10.1186/2008-6970-4-19.
- Khaldi, M., Ronse, G., André, C., Blanpain-Avet, P., Bouvier, L., Six, T., Bornaz, S., Croguennec, T., Jeantet, R., & Delaplace, G. (2015). Denaturation kinetics of whey protein isolate solutions and fouling mass distribution in a plate heat exchanger. *International Journal of Chemical Engineering*. doi:10.1155/2015/139638.
- Kong, F., Tang, J., Rasco, B., & Crapo, C. (2007a). Kinetics of salmon quality changes during thermal processing. *Journal of Food Engineering*, 83, 510–520.
- Kong, F., Tang, J., Rasco, B., Crapo, C., & Smiley, S. (2007b). Quality changes of salmon (*Oncorhynchus gorbuscha*) muscle during thermal processing. *Journal of Food Science*, 72(2), 103–111.
- Kirschner, C., Ofstad, R., Skarpeid, H. J., Host, V., & Kohler, A. (2004). Monitoring of denaturation processes in aged beef loin by Fourier transform infrared microspectroscopy. *Journal of Agricultural and Food Chemistry*, 52, 3920–3929.
- Ling, B., Tang, J., Kong, F., Mitcham, E. J., & Wang, S. (2015). Kinetics of food quality changes during thermal processing: a review. *Food and Bioprocess Technology*, 8, 343–358.
- Ma, C., & Harwalkar, V. R. (1991). Thermal analysis of food proteins. *Advances in Food and Nutrition Research*, 35, 317–366.
- Mao, W., Li, X., Fukuoka, M., Liu, S., Ji, H., & Sakai, N. (2016). Study of Ca²⁺-ATPase activity and solubility in the whole Kuruma prawn (*Marsupenaeus japonicas*) meat during heating: based on the kinetics analysis of myofibril protein thermal denaturation. *Food and Bioprocess Technology*, 9(9), 1511–1520.
- Niu, L., Rasco, B., Tang, J., Lai, K., & Huang, Y. (2015). Relationship of changes in quality attributes and protein solubility of ground beef under pasteurization conditions. *LWT-Food Science and Technology*. doi:10.1016/j.lwt.2014.11.016.
- Ofstad, R., Kidman, S., & Hermansson, A. M. (1996). Ultramicroscopical structures and liquid loss in heated cod (*Gadus morhua*) and salmon (*Salmo salar*) muscle. *Journal of the Science of Food and Agriculture*, 72(3), 337–347.
- Ojagh, S. M., Nunez-Flores, R., Lopez-Caballero, M. E., Montero, M. P., & Gomez-Guillen, M. C. (2011). Lessening of high pressure induced changes in Atlantic salmon muscle by the combined use of a fish gelatin-lignin film. *Food Chemistry*, 125, 595–606.
- Ovissipour, M., Rasco, B., Tang, J., & Sablani, S. S. (2013). Kinetics of quality changes in whole blue mussel (*Mytilus edulis*) during pasteurization. *Food Research International*, 53, 141–148.
- Palka, K., & Daun, H. (1999). Changes in texture, cooking losses, and myofibrillar structure of bovine *M. semitendinosus* during heating. *Meat Science*, 51(3), 237–243.
- Paredi, M. E., Tomas, M. C., Añon, M. C., & Crupkin, M. (1998). Thermal stability of myofibrillar protein from smooth and striated muscles of scallop (*Chlamys tehuellchus*): a differential scanning calorimetric study. *Journal of Agricultural and Food Chemistry*, 46, 3971–3976.
- Rattanasatheir, N., Benjakul, S., Visessanguan, W., & Kijroongrojana, K. (2008). Properties, translucence, and microstructure of Pacific White shrimp treated with mixed phosphates as affected by freshness and deveining. *Journal of Food Science*, 73(1), 31–40.
- Skipnes, D., Ostby, M. L., & Hendrickx, M. E. (2007). A method for characterising cook loss and water holding capacity in heat treated cod (*Gadus morhua*) muscle. *Journal of Food Engineering*, 80, 1078–1085.
- Skipnes, D., Van der Plancken, I., Van Loey, A., & Hendrickx, M. (2008). Kinetics of heat denaturation of proteins from farmed Atlantic cod (*Gadus morhua*). *Journal of Food Engineering*, 85(1), 51–58.
- Skipnes, D., Johnson, S. O., Skara, T., Sivertsik, M., & Lekang, O. (2011). Optimization of heat processing of farmed Atlantic cod (*Gadus morhua*) muscle with respect of cook loss, water holding capacity, color, and texture. *Journal of Aquatic Food Product Technologies*, 20, 331–340.
- Verhaeghe, T., Vlaemynck, G., Block, J. D., Van Weyenberg, S., Braeckman, R., & Hendricks, M. (2016). Kinetics of heat induced muscle protein denaturation of brown shrimp (*Crangon crangon*). *Journal of Food Engineering*, 191, 88–94.
- Wang, Y., Wig, T. D., Tang, J., & Hallberg, L. M. (2003). Dielectric properties of foods relevant to RF and microwave pasteurization and sterilization. *Journal of Food Engineering*, 57, 257–268.
- Wang, Y., Tang, J., Rasco, B., Kong, F., & Wang, S. (2008). Dielectric properties of salmon fillets as a functional of temperature and composition. *Journal of Food Engineering*, 87, 2367–2246.
- Wang, J., Tang, J., Wang, Y., & Swanson, B. (2009). Dielectric properties of egg whites and whole eggs as influenced by thermal treatments. *LWT-Food Science and Technology*, 42, 1204–1212.
- Whistler, R. L., & Daniel, J. R. (1985). Carbohydrates. In O. R. Fennema (Ed.), *Food chemistry* (pp. 98–99). Marcel Dekker.
- Wolz, M., & Kulozik, U. (2015). Thermal denaturation kinetics of whey proteins at high protein concentrations. *International Dairy Journal*, 49, 95–101.
- Wu, Z., Bertram, H. C., Kohler, A., Bocker, U., Ofstad, R., & Andersen, H. J. (2006). Influence of aging and salting on protein secondary structures and water distribution in uncooked and cooked pork. A combined FT-IR microspectroscopy and ¹H NMR relaxometry study. *Journal of Agricultural and Food Chemistry*, 54, 8589–8597.
- Yan, Y.-B., Wang, Q., He, H.-W., & Zhou, H.-M. (2004). Protein thermal aggregation involves distinct regions: sequential events in the heat-induced unfolding and aggregation of hemoglobin. *Biophysical Journal*, 86, 1682–1690.
- Yoon, W. B., Gunasekaran, S., & Park, J. W. (2004). Characterization of thermorheological behavior of Alaska Pollock and Pacific Whiting surimi. *Journal of Food Science*, 69(7), 338–343.